Hollow Fiber Membrane Decorated with Ag/MWNTs: Toward Effective Water Disinfection and Biofouling Control

Poernomo Gunawan,[†] Cong Guan,[†] Xianghua Song,[†] Quanyuan Zhang,[†] Susanna Su Jan Leong,[†] Chuyang Tang,[‡] Yuan Chen,[†] Mary B. Chan-Park,[†] Matthew Wook Chang,[†] Kean Wang,[†] and Rong Xu[†,*]

[†]School of Chemical and Biomedical Engineering, Nanyang Technological University, 62 Nanyang Drive, Singapore 637459, and [‡]School of Civil & Environmental Engineering, Nanyang Technological University, 50 Nanyang Avenue, Singapore 639798

ABSTRACT

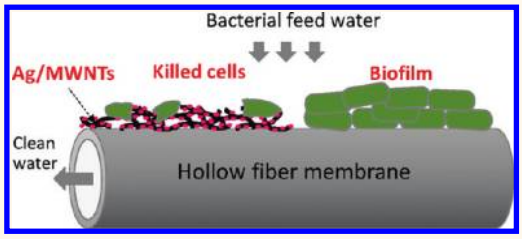

The currently applied disinfection methods during water treatment provide effective solutions to kill pathogens, but also generate harmful byproducts, which are required to be treated with additional efforts. In this work, an alternative and safer water disinfection system consisting of silver nanoparticle/multiwalled carbon nanotubes (Ag/MWNTs) coated on a polyacrylonitrile (PAN) hollow fiber membrane, Ag/MWNTs/PAN, has been developed. Silver nanoparticles of controlled sizes were coated on polyethylene glycol-grafted MWNTs. Ag/MWNTs were then covalently coated on the external surface of a chemically modified PAN hollow fiber membrane to act as a disinfection barrier. A continuous filtration test using *E. coli* containing feedwater was conducted for the pristine PAN and Ag/MWNTs/PAN composite membranes. The Ag/MWNT coating significantly enhanced the antimicrobial activities and antifouling properties of the membrane against *E. coli*. Under the continuous filtration mode using *E. coli* feedwater, the relative flux drop over Ag/MWNTs/PAN was 6%, which was significantly lower than that over the pristine PAN (55%) at 20 h of filtration. The presence of the Ag/MWNT disinfection layer effectively inhibited the growth of bacteria in the filtration module and prevented the formation of biofilm on the surface of the membrane. Such distinctive antimicrobial properties of the composite membrane is attributed to the proper dispersion of silver nanoparticles on the external surface of the membrane, leading to direct contact with bacterium cells.

KEYWORDS: silver · carbon nanotubes · composites · membranes · antimicrobial · biofilm

Pathogenic microorganisms present in natural and used water pose a serious threat to public health if not removed during water treatment. With increasing demands for higher quality water to satisfy escalating public and industrial needs, the generation of pathogen-free clean water with few byproducts has gained significant attention.[1,2] Membrane filtration especially using hollow fiber membranes represents an important and advanced water purification and desalination process. However, the lack of bactericidal properties of current filtration membranes allows membrane biofouling, which necessitates frequent backflushing, chemical treatment, and even membrane replacement.

Colloidal silver has been approved by the U.S. Environmental Protection Agency as a disinfectant for hospitals and medical centers. Colloidal silver at a concentration of a few ppm has been found effective in killing numerous infectious bacteria.[3−7] The bactericidal mechanism of Ag^+ ions has been well studied and understood. The interaction of Ag^+ ions with thiol groups (S−H) of cysteine and other compounds and the formation of Ag−S bonds can cause detrimental effects to cells by damaging proteins, interrupting the electron transport pathway, and dimerizing DNA.[3,8,9] Although the exact antibacterial mechanism of colloidal silver nanoparticles remains unclear, it has been shown that silver nanoparticles themselves are active through a contact-inhibition mode. It was suspected that silver nanoparticles may cause an increase in cell membrane permeability by their direct incorporation into the cell membrane and the subsequent formation of permeable pits. This then leads to osmotic collapse and a release of intracellular materials.[10−13] In addition, various research groups have reported that the toxicity of silver nanoparticles is influenced by the particle size and morphologies.[6,10,12] Silver nanoparticles of less than 10 nm and with ⟨111⟩ facets exposed have been found more effective.

Immobilization of silver nanoparticles into appropriate matrixes could offer a potential solution to the development of a disinfection system with good reliability and ease of operation.[14,15] Several water

* Address correspondence to rxu@ntu.edu.sg.

Received for review October 8, 2011 and accepted November 13, 2011.

Published online November 13, 2011
10.1021/nn2038725

filtration membranes incorporated with silver nanoparticles have been reported. In these studies, the mixed-matrix membranes were formed by either *in situ* reduction of silver nitrate that was added to the polymer solution at the beginning or by blending *ex situ* prepared silver nanoparticles into the polymer solutions, both followed by the phase inversion process.[16−20] Silver nanoparticles were entrapped and distributed in the entire structure of the membrane in these systems. Under continuous filtration, Taurozzi *et al*. reported that the silver/polysulfone membrane did not exhibit a significant difference in biofilm inhibition compared to the unmodified membrane because the leached silver ions were convectively carried away from the bacteria on the membrane surface to the permeate side of the membrane.[18] More recently, Mauter *et al*. reported the grafting of polyethyleneimine-coated silver nanoparticles on the surface of a plasma-treated polysulfone membrane. They showed that the active layer exhibited excellent antimicrobial activity against *Escherichia coli*.[21] Such findings indicate that it is important to have the silver nanoparticles located at the membrane/water interface to allow a direct contact between silver and bacteria cells for optimal performance.

In this work, we developed a nanocomposite coating layer based on multiwalled carbon nanotubes (MWNTs) and silver nanoparticles (Ag/MWNTs) on the surface of a commercial hollow fiber polyacrylonitrile (PAN) membrane. Besides functioning as the support for silver nanoparticles, the nanoscale diameter and one-dimensional morphology of MWNTs allow an open network structure on the membrane surface to minimize the impact on water flux and also facilitate the contact of silver nanoparticles by pathogens. Both the deposition of silver nanoparticles on MWNTs and the coating of Ag/MWNTs on PAN were achieved by covalent grafting to attain strong binding among various components (Scheme 1). It has been shown that the Ag/MWNTs disinfection layer coated on the external surface is effective in killing bacteria and controlling biofilm growth under the filtration mode. The unique system developed in this work could be potentially used as a disinfection system for antimicrobial water treatment. The methodology may also be extended to other disinfectant/membrane systems for wide applications.

RESULTS AND DISCUSSION

Characteristics of Ag/MWNTs. Multiwalled carbon nanotubes (MWNTs) are reported as suitable materials for immobilization of nanoparticles for various advanced applications such as sensing, catalysis, and electrocatalysis.[22−24] Silver nanoparticles immobilized on MWNTs (Ag/MWNTs) have been demonstrated with good antimicrobial properties against bacteria.[25,26] Ag/MWNTs can be synthesized by various methods such as *in situ* deposition on modified carbon nanotubes,[27,28] electrodeposition,[29] chemical reduction,[30] and microwave heating.[31] Nonetheless, formation of well-dispersed and uniformly sized silver nanoparticles by facile routes is still a challenging task. In this work, MWTNs were first grafted with polyethylene glycol (PEG), which played dual roles of hydrophilicity enhancement of MWNTs and reducing sites for formation of well-dispersed silver nanoparticles. The preparation of Ag/MWNTs was according to the steps shown in Scheme 1(A−D). After carboxylation of MWNTs, 1,6-hexamethylene diisocyanate was used as a linker between the carboxylate group and PEG. The pristine MWNTs, carboxylated MWNTs (MWNTs-COOH), and PEG-grafted MWNTs (MWNTs-PEG) were characterized with Fourier transform infrared (FTIR) as shown in Figure 1. The pristine MWNTs exhibit bands around 1640 and 3400 cm^{-1}, which can be assigned to the bending mode and the −OH stretching vibration of adsorbed water molecules, respectively.[32] After oxidation with the concentrated acids, there appears a shoulder at 1720 cm^{-1}, which is attributed to the carboxylic acid group in MWNTs-COOH. The peaks at 2909 and 2962 cm^{-1} in the FTIR spectrum of MWNTs-COOH can be assigned to the stretching vibration of the C−H group. Similar absorption peaks for acid-oxidized carbon nanotubes and carbon nanofibers have also been reported by other groups.[33,34] The presence of CH_2/CH_3 groups in nanotubes and carbon nanofibers was attributed to defects generated in the graphitic structure of carbon during their production. It is also likely that acid treatment creates such defects. Upon grafting with PEG, the stretching mode of C−C−O is evident by the appearance of the band at 1090 cm^{-1}.[32]

PEG of suitable chain lengths in the solution was reported capable of reducing silver ions to metallic silver nanoparticles accompanied by oxidation of the hydroxyl group of PEG to aldehyde.[35] It is believed that the grafted PEG on MWNTs in the current system plays a similar role in reduction of silver ions to silver nanoparticles of controlled sizes and at the same time binding them on the surface of MWNTs. The X-ray diffraction (XRD) pattern of the resulting sample is shown in Figure 2A. The broad peak at around 26° is assigned to the (002) plane of MWNTs,[25] while the remaining peaks can be indexed to the cubic phased metallic silver (PDF no. 001-1167), as indicated by the line pattern. The strongest peak at 38.1° correlates to the (111) diffraction plane. As shown in the transmission electron microscopy (TEM) images (Figure 2B and C), an excellent dispersion of silver nanoparticles sized around 2−5 nm on MWNTs can be observed. Although the carboxylic acid groups of acid-treated MWNTs can also function as the reduction sites,[27] their control over the particle size and dispersion is limited on the basis of the literature results and also our control experiment (data not shown). The function of PEG can be clearly distinguished on the basis of our studies. A high-resolution image of an individual nanoparticle (Figure 2D) shows the lattice distance of 0.230 nm, which

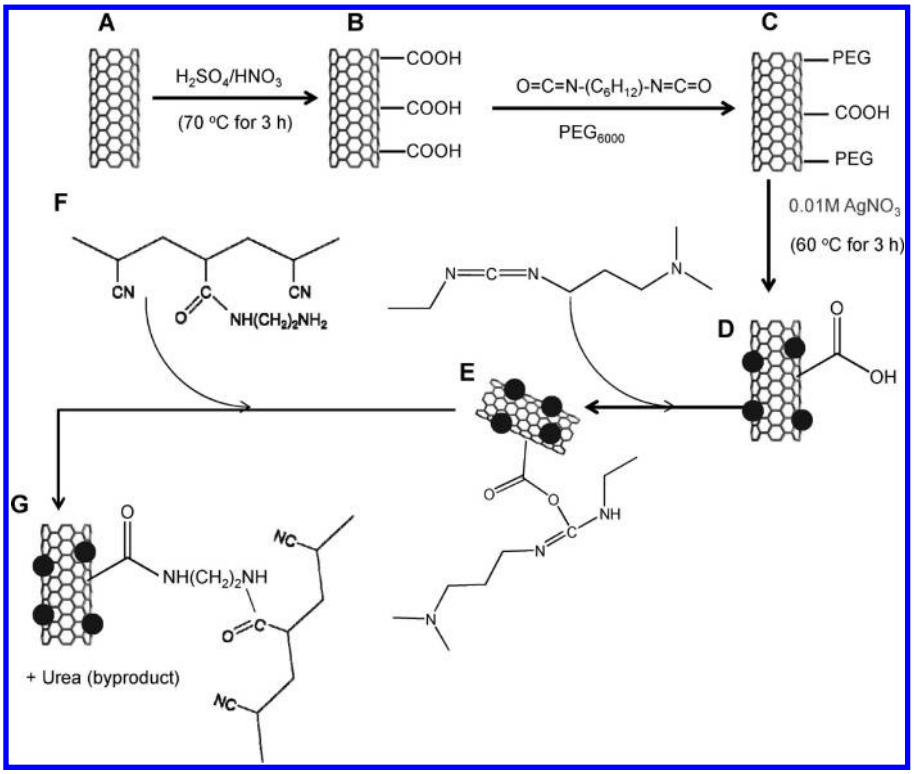

Scheme 1. Proposed formation pathway of an Ag/MWNT-decorated PAN composite membrane (Ag/MWNTs/PAN) (G): (A) pristine MWNTs, (B) acid-treated MWNTs (MWNTs-COOH), (C) PEG-grafted MWNTs (MWNTs-PEG), (D) silver nanoparticle-deposited MWNTs (Ag/MWNTs), (E) 1-ethyl-3-(3-dimethylaminopropyl) carbodiimide hydrochloride (EDC)-linked Ag/MWNT intermediate, and (F) ethylene diamine (EDA)-modified PAN (PAN-EDA).

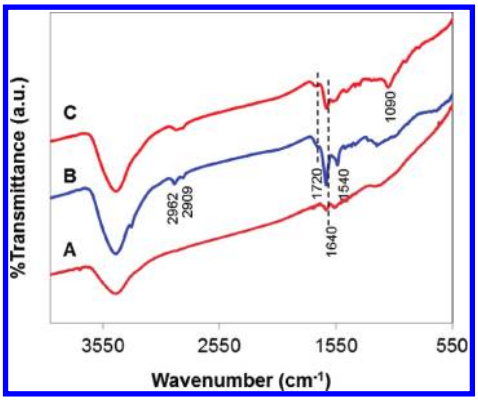

Figure 1. FTIR spectra of (A) prinstine MWNTs, (B) MWNTs-COOH, and (C) MWNTs-PEG.

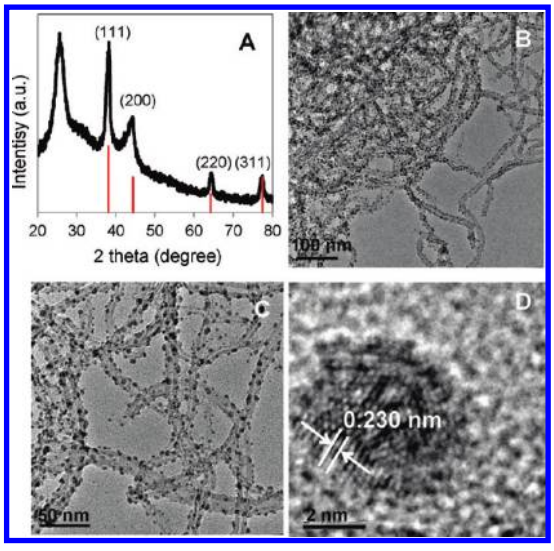

Figure 2. (A) XRD pattern (the line pattern indicates the standard pattern of metallic silver with PDF no. 001-1167). (B and C) TEM and (D) HRTEM images of Ag/MWNTs.

is in good agreement with that of the (111) plane distance. The weight percentage of silver in the composite was determined to be about 2.45% using inductively coupled plasma (ICP) analysis.

The thermogravimetric analysis (TGA) results of pristine MWNTs, MWNTs-COOH, and MWNTs-PEG are shown in Figure 3. On the basis of the weight loss data at 600 °C, it can be estimated that roughly 16.9% of carbon of MWNTs is oxidized to −COOH and 18.7% of −COOH is further grafted with PEG.[36] The FTIR spectrum of MWNTs-PEG (Figure 1C) shows consistent evidence that the carboxylic acid group is still present after PEG grafting, as indicated by the absorption at 1720 cm^{-1}. Hence, the remaining free −COOH on the surface of MWNTs-PEG is proposed to be responsible for the attachment of Ag/MWNTs to EDA-modified PAN, as proposed in Scheme 1.

Properties of Ag/MWNTs/PAN Composite Membrane. The pristine PAN hollow fiber membrane has a typical asymmetric pore structure with long finger-like pores (Figure

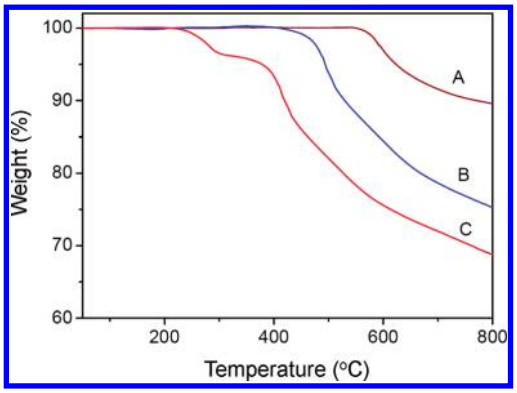

Figure 3. TGA results of (A) prinstine MWNTs, (B) MWNTs-COOH, and (C) MWNTs-PEG.

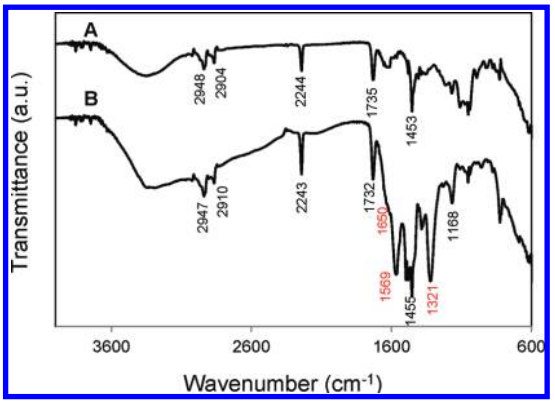

Figure 4. ATR-FTIR spectra of (A) pristine PAN and (B) PAN-EDA.

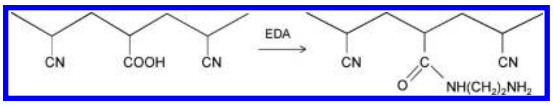

Scheme 2. Proposed aminolysis reaction of partially hydrolyzed PAN with EDA

S1A and S1B) and a dense and smooth outer layer (Figure S1B and S1C). After treatment with a 20 vol % aqueous solution of EDA, the outer surface of EDA-treated PAN (PAN-EDA) is no longer smooth and patches of surface defects can be observed (Figure S1D), although the large finger-like pore structure is unaffected (not shown).

The chemical modification of PAN by EDA was evidenced from ATR-FTIR spectra shown in Figure 4. In Figure 4A, the characteristic vibration of the nitrile group (C≡N) appears at 2244 cm^{-1}. The peaks at 2904 and 2948 cm^{-1} are assigned to the stretching vibration of the CH_2 group of PAN, while the peak at 1453 cm^{-1} is due to the bending vibration of the same group.[37] The additional peaks at 1735 cm^{-1} in the spectrum of PAN (compared to that of the fresh PAN powder in Figure S2) can be attributed to the vibration of C═O of the carboxylic group, indicating that PAN has been partially hydrolyzed after being soaked in water before modification with EDA. Similar results have been reported in the literature.[38] In the spectrum of PAN-EDA (Figure 4B), the above peaks remain at similar positions. Additional vibrations can be found at 1650, 1569, and 1321 cm^{-1}. The first two can be assigned to amide I (C═O stretching) and amide II (NH deformation), respectively.[39,40] The peak at 1321 cm^{-1} is due to the bending vibration of the CH_2 group in EDA. On the basis of such results, the proposed reaction pathway of PAN modification by EDA is *via* an aminolysis reaction of partially hydrolyzed PAN, as shown in Scheme 2.

Physisorption by liquid nitrogen was performed to measure the surface area and pore size of both pristine PAN and PAN-EDA. The surface area of PAN was increased from 39.6 m^2/g to 46.4 m^2/g after EDA treatment. The pore size distribution of the dense layer is shown in Figure S3. The pristine PAN membrane (Figure S3A) has a few distinct pore sizes centered at 2.7, 3.4, and 4.2 nm, while PAN-EDA exhibits a broad pore size distribution in the range 2−5 nm (Figure S3B). These results indicate that the pore structure at the outer surface layer was slightly modified after the chemical treatment by 20 vol % EDA. Consequently, the initial flux measured using deionized water for PAN-EDA was 220 $L/m^2/h/bar$, which was about 25% lower than that of the pristine PAN. Other chemical treatments using aqueous NaOH solution (1.0 M), HCl solution (1.0 M), and more concentrated EDA solutions (50 and 99 vol %) were also used to modify PAN in this work. However, all these treatments resulted in more than 90% decrease in the initial flux, which should be attributed to a more severe influence on the pore structure. Research effort is under way to develop alternative methods to produce surface-activated membranes without compromising on water flux.

Attachment of Ag/MWNTs on PAN-EDA was carried out with the assistance of 1-ethyl-3-(3-dimethylaminopropyl) carbodiimide hydrochloride (EDC) as an amide-forming agent (Scheme 1D−G). The addition of EDC facilitates the amidation reaction between the carboxylic acid on Ag/MWNTs and the amine group on PAN-EDA. Consequently, Ag/MWNTs can be stably grafted on the surface of PAN by covalent linkage. Two control samples were prepared to investigate the effects of EDA and EDC. The first sample was obtained by reacting pristine PAN with Ag/MWNTs in the presence of EDC, and the second sample was prepared by reacting PAN-EDA with Ag/MWNTs in the absence of EDC. The SEM images of Ag/MWNTs/PAN are shown in Figure 5. It can be clearly observed that a significant amount of Ag/MWNTs was attached to the surface of PAN. On the other hand, there is no evidence of attachment of Ag/MWNTs in both control samples (Figure S4). Such results support the proposed reaction schemes in which the modification of PAN by EDA and the presence of EDC as a linking agent are both important toward the formation of Ag/MWNTs/PAN composite membranes.

The average pore size of the dense layer of PAN-EDA was measured to be about 3 nm by the N_2 adsorption method. Since the average diameter of

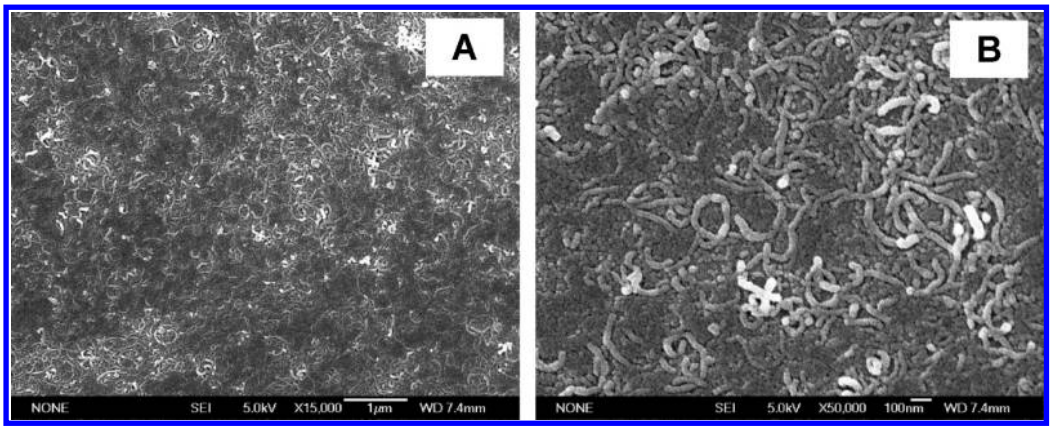

Figure 5. SEM images of the surface of a Ag/MWNTs/PAN composite membrane at (A) low and (B) high magnifications.

MWNTs used is around 11 nm, the coating will be largely on the external surface of the membrane in a mesh-like form, as shown in Figure 5. Although the surface of the pristine MWNTs consisting of a graphitic carbon layer is hydrophobic, functionalization of MWNTs with carboxylic groups and PEG greatly increases the hydrophilicity of the resulting Ag/MWNTs. In fact, the Ag/MWNTs/PAN composite membrane has a similar hydrophilicity to that of the pristine PAN, with their contact angles measured to be 76.5° and 79.9°, respectively. As such, the coating does not add significant hydraulic resistance to the membrane. The initial flux of the Ag/MWNTs/PAN composite membrane drops only about 7% to 205 L/m^2/h/bar compared with that of PAN-EDA.

Antimicrobial Properties of Ag/MWNTs/PAN Composite Membrane. In this work, *Escherichia coli* (*E. coli*) was used as a model bacterium to investigate the antimicrobial and antifouling properties of the composite membrane due to a growing concern over the infections worldwide caused by this bacterium.[41] A solution of HEPES/glucose with a constant pH of 7.0 was used as the medium for the bacterium-containing feedwater during filtration. This medium can provide a nutritious environment (by glucose) to minimize bacterium death, since a high concentration of viable cells in the feedwater is necessary during filtration. To obtain the effect of the medium on the flux, a control permeation test was conducted over the pristine PAN membrane with the medium itself as the feed. Figure 6A shows that the flux drop due to the medium is not significant, with about 8% during the first 5 h and another 4% during the remaining 15 h. The initial drop could be due to the adsorption of glucose and/or the ionic species in the medium onto the pores of PAN, which slightly affects the hydrodynamics of the membrane. The presence of *E. coli* in the feedwater affected the flux of the pristine PAN membrane significantly. As shown in Figure 6A, the flux dropped 55% from 260 to 117 L/h/m^2/bar in 20 h, indicating that the pristine PAN membrane can be easily fouled under the present conditions. In contrast, the Ag/MWNTs/PAN composite membrane shows a much improved fouling resistance. The flux drop was only 6% from 205 to 193 L/h/m^2/bar, which could be mainly due to the effect of the medium.

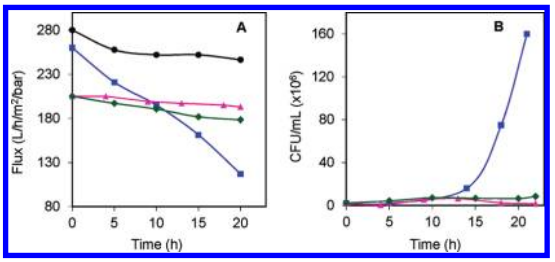

Figure 6. Continuous filtration test: (A) the flux change using *E. coli*-containing feedwater and (B) viable *E. coli* cell concentration in the reject water. (●) Control permeation test of pristine PAN using the medium without *E. coli*, (■) pristine PAN, (▲) Ag/MWNTs/PAN, (♦) Ag/MWNTs/PAN after soaking in deionized water for 14 d.

It is notable that no bacterium cells were found in the permeate water samples for both pristine and composite membranes, as the external surface of the PAN membrane with a pore size of a few nanometers is effective in filtering micrometer-sized bacterium cells. Hence, all cells were trapped inside the filtration module, and they could further grow or be killed depending on the properties of the membrane. The population of the living cells in the reject water was measured during filtration. As shown in Figure 6B, the concentration of living *E. coli* cells increased to about 80-fold (starting concentration at about 2 $\times$ 10^6 cfu) in the reject water at 21 h of filtration when the pristine PAN membrane was used. In contrast, the composite membrane with the Ag/MWNTs disinfection layer can effectively inhibit the bacterial growth within the test duration of 22 h. No significant increase in living *E. coli* cell concentration was found.

The above results are well correlated to the biofilm inhibition properties of the membranes. As shown in Figure 7A, dense and complex biofilm was formed on the pristine PAN membrane after the filtration test in about one day. The presence of biofilm on the membrane severely affected the water flux, as shown in Figure 6A. In contrast, only scattered cells were

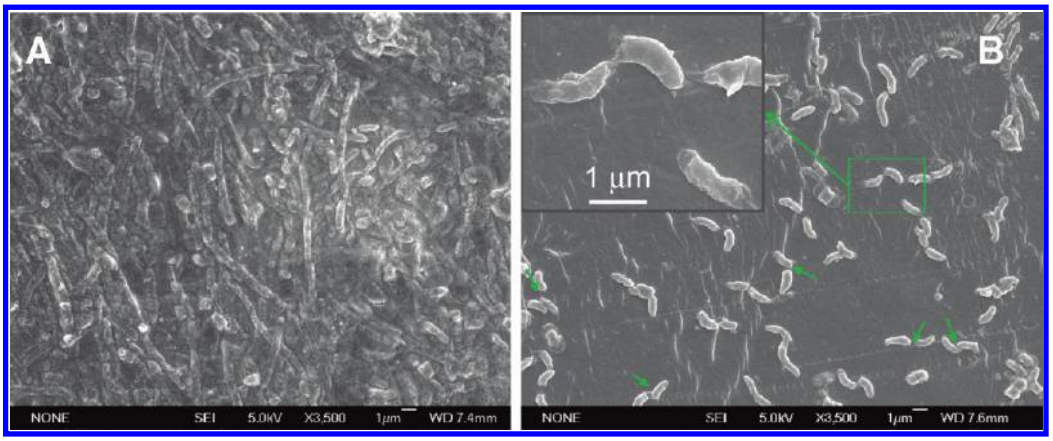

Figure 7. SEM images of the pristine (A) PAN membrane and (B) Ag/MWNTs/PAN composite membrane after 22 h filtration test using *E. coli*-containing feedwater.

observed on the Ag/MWNTs/PAN composite membrane (Figure 7B). Furthermore, the majority of *E. coli* cells found on the composite membrane were shown with damaged cell walls (as indicated by the arrows for some representative cells and the magnified image in Figure 7B inset), indicating that the cell membranes were disrupted, which is probably due to the direct contact between the cells and silver nanoparticles.[10−12] Taurozzi *et al*. showed that under the flow test the silver-embedded polysulfone membrane was not effective in reducing biofouling by *E. coli*.[18] Our previous study has shown that MWNTs-COOH exhibited a much lower efficacy in killing bacteria (50% kill for *E. coli*) than Ag/MWNTs (>99%) under the same conditions.[25] Our other work consistently showed that both MWNTs and MWNTs-PEG have low antimicrobial activities and biofilm inhibition ability.[36] The distinctively high efficacy of our composite membrane on biofouling control in this work lies in the proper dispersion of silver nanoparticles on the surface of the membrane for direct contact with bacterial cells. After 600 L/m^2 of filtration, the silver loss in the composite membrane was determined to be about 22%. The concentration of leached Ag^+ ions in the permeate water was measured to be always less than 10 ppb, which is below the allowable maximum silver concentration in drinking water (around 50 ppb). Silver loss from the surface was commonly reported by others, due to their easy accessibility to the water.[16,17,19] To test the stability of our membrane, the Ag/MWNTs/PAN composite membrane was soaked in deionized water for two weeks followed by filtration under the same test conditions. Although about 60% of silver was lost from the membrane, their antimicrobial properties did not deteriorate much. As shown in Figure 6A, the flux drop was increased from 6% to 13%, which was still much better than that of the pristine membrane. There was also no significant increase in the concentration of the living cells in the reject water (Figure 6B). More research work is underway to achieve a better durability of the system as well as effective silver regeneration.

CONCLUSIONS

In summary, a novel water disinfection system consisting of silver nanoparticle/multiwalled carbon nanotubes (Ag/MWNTs) coated on a PAN hollow fiber membrane, Ag/MWNTs/PAN, was developed. Silver nanoparticles of controlled sizes (2−5 nm) were successfully coated on MWNTs that were first modified with PEG. PEG not only acted as a reducing agent for conversion of silver ions to metallic silver nanoparticles, leading to their immobilization on MWNTs, but also increased the hydrophilicity of MWNTs for less adverse effect on the flux of the resulting composite membrane. Ag/MWNTs were covalently coated on the external surface (*i.e.*, the dense layer) of a PAN hollow fiber membrane. The filtration study using the feedwater containing *E. coli* was conducted for pristine PAN and Ag/MWNTs/PAN membranes. It was found that the Ag/MWNT coating significantly enhanced the antimicrobial activities and antifouling properties of the membrane. A much lower degree of fouling was observed on the Ag/MWNTs/PAN membrane. As a result, the relative flux drop over Ag/MWNTs/PAN was significantly smaller than that over the pristine PAN. It is believed that Ag^+ ions released from the Ag/MWNTs layer as well as the direct contact between the silver nanoparticles and the cells caused effective killing of the bacteria and inhibition of biofouling.

EXPERIMENTAL SECTION

Modification of PAN Hollow Fiber Membrane by EDA. The properties of PAN hollow fiber membranes (Ultra-Flo Pte Ltd., Singapore) are listed in Table S1. PAN was soaked in deionized water after arrival. The amination of PAN was conducted by immersing the wet PAN membranes (250 mm in length) in 100 mL of an aqueous solution of 20 vol % of ethylene diamine (EDA, Alfa

Aesar, 99%). The mixture was shaken at 100 rpm at room temperature for 24 h. The modified PAN membranes were rinsed with deionized water several times until the pH of the rinsed water reached about 7.0. The membranes denoted as PAN-EDA were kept wet for further use.

Preparation of Ag/MWNTs Nanocomposite. MWNTs (CNano Technology Ltd., purity: >95%, average length: 10 μm, average diameter: 11 nm) were first carboxylated by treatment with concentrated H_2SO_4 (Merck, 98%) and HNO_3 (Honeywell, 69%), as described in our previous work.[25] To functionalize MWNTs-COOH with polyethylene glycol, 100 mg of dried MWNTs-COOH was ultrasonicated in 60 mL of acetone for 30 min followed by purging with N_2 gas at 60 mL/min at 50 °C for another 30 min. Subsequently, 0.2 mL (1.25 mmol) of 1,6-hexamethylene diisocyanate (Fluka, 99%) was added into the MWNTs-COOH suspension, and the mixture was stirred at 50 °C for 2 h. Afterward, 9 g (1.5 mmol) of PEG (molecular weight: 6000, Alfa Aesar, >99%) was added into the suspension followed by stirring for another 2 h at the same temperature. N_2 purging was carried out throughout the reaction, and a water condenser was mounted on top of the flask. The resulting product (MWNTs-PEG) was first washed with acetone followed with deionized water several times and then dried under vacuum overnight for further loading of silver nanoparticles. Silver nanoparticles were loaded onto MWNTs-PEG through reduction of Ag^+ ions by PEG grafted on the surface of the MWNTs. Briefly, 50 mg of MWNTs-PEG was ultrasonicated in 10 mL of deionized water for 30 min. Then, 20 mL of 0.01 M $AgNO_3$ (BDH, 99%) aqueous solution was added into the MWNTs-PEG suspension. The mixture was heated to 60 °C and maintained at this temperature for 3 h under stirring. The resulting product, denoted as Ag/MWNTs, was washed twice with deionized water and then dried under vacuum overnight.

Grafting of Ag/MWNTs on a PAN-EDA Hollow Fiber Membrane. PAN-EDA hollow fibers were immersed in a suspension of 25 mg of Ag/MWNTs in 100 mL of deionized water. Both ends of the hollow fiber membranes were lifted above the surface of the suspension in order to prevent the entrance of Ag/MWNTs into the interior space of the hollow fibers. Then, 200 mg of 1-ethyl-3-(3-dimethylaminopropyl) carbodiimide hydrochloride (Acros, 99%) was added, and the mixture was shaken gently at room temperature for 16 h. The membranes attached with Ag/MWNTs, denoted as Ag/MWNTs/PAN, were then rinsed with deionized water and kept wet for subsequent filtration and antimicrobial testing.

Materials Characterization. The powder X-ray diffraction pattern of Ag/MWNTs was recorded in a Bruker AXS D8 X-ray diffractometer with Cu Kα (λ = 1.5406 Å) radiation at 40 kV and 20 mA. Fourier transform infrared spectra were obtained on a Digilab FTS 3100 FTIR with a 4 cm^{-1} resolution and in the range 400−4000 cm^{-1} using a standard KBr disk technique. Particle size and morphology were observed using JEOL 3010 transmission electron microscopy. Thermogravimetric analysis was carried out by heating the dry powder samples at a rate of 10 °C/min with nitrogen flow at 200 mL/min over 25−800 °C in a TA Instruments SDT Q600. The functional groups of the pristine and modified membrane were studied using ATR-IR on a Perkin-Elmer Spectrum One FTIR spectrometer. The morphologies of the membranes were examined by SEM (JEOL JSM 6700F field emission). The surface area and pore size of the membrane were measured by nitrogen physisorption using Quantachrome Autosorb 6B. The contact angle measurement of water on thoroughly dried membranes was conducted in a FTA 200 (First Ten Angstroms, Portsmouth, VA, USA). The percentages of silver in Ag/MWNTs and Ag/MWNTs/PAN were determined using inductively coupled plasma atomic emission spectroscopy (ICP-AES) in a Perkin-Elmer ICP Optima 2000DV after dissolving silver in dilute solutions of HNO_3.

Filtration Module Setup and Permeation Test. A bench-scale test module was set up to evaluate the permeation and antimicrobial properties of a Ag/MWNTs/PAN composite membrane. The schematic diagram of the module is shown in Figure S5. The fibers were sealed at one end with epoxy glue. The wall of the module was made of acrylic glass pipe with an outer diameter of 25.4 mm. Before the permeation test, the module was pressurized at 2.0 bar for leakage checking. The module was operated with in outside-in mode. Deionized water was permeated through the membrane module for 30 min for initial flux measurement, during which the flow rate was fixed at 5 mL/min. The permeate volume was measured to calculate the flux according to eq 1.

$$Q = A \times flux \times P \quad (1)$$

where Q is the volumetric flow rate, A is the total surface area of the hollow fibers, and P is the transmembrane pressure (TMP). TMP was measured by a digital pressures gauge (GE Druck DPI 104, Accuracy: 0.05% of full span).

Filtration Test of a Ag/MWNTs/PAN Composite Membrane Using Bacterial Water. The target *Escherichia coli* (*E. coli*) bacterium was cultured to a midlog phase in Luria−Bertani (LB) broth (Difco LB Broth, Miller) at 37 °C. The cells were harvested by centrifugation, washed, and resuspended in a mixed solution of HEPES buffer (10 mM) and glucose (1 wt %) with the cell concentration approximately at 10^6 colony forming units (cfu's) per mL. The resulting mixture was used as the feedwater for the filtration study. The permeation test for the Ag/MWNTs/PAN composite membrane and the pristine PAN membrane was performed at room temperature under the same conditions. The flow rate of bacteria-containing feedwater was fixed at 24 L/h/m^2. The flux was obtained for both membranes for comparison. The concentration of living bacterium cells inside the filtration module (*i.e.*, in the reject water) and in the filtrate was determined by the colony-counting method. Both the pristine and Ag/MWNTs/PAN composite membranes were examined by FESEM (JEOL JSM 6700F field emission) after the filtration test. Prior to the analysis, all membrane samples were subjected to freeze-drying under vacuum at −50 °C for 12 h.

Acknowledgment. This research was funded by Environment and Water Industry Programme Office (EWI), National Research Foundation Singapore, through project no. 0802-IRIS-12.

Supporting Information Available: Properties of PAN membrane, bench-scale filtration system, and additional SEM, pore size distribution, and FTIR results. This material is available free of charge *via* the Internet at http://pubs.acs.org.

REFERENCES AND NOTES

1. Krasner, S. W.; Weinberg, H. S.; Richardson, S. D.; Pastor, S. J.; Chinn, R.; Sclimenti, M. J.; Onstad, G. D.; Thruston, A. D. Occurrence of a New Generation of Disinfection Byproducts. *Environ. Sci. Technol.* **2006**, *40*, 7175–7185.
2. Xie, Y. *Disinfection Byproducts in Drinking Water: Formation, Analysis, and Control*; CRC Press: Boca Raton, FL, 2003.
3. Russell, A. D.; Hugo, W. B. Antimicrobial Activity and Action of Silver. *Prog. Med. Chem.* **1994**, *31*, 351–370.
4. Alt, V.; Bechert, T.; Steinrucke, P.; Wagener, M.; Seidel, P.; Dingeldein, E.; Domann, E.; Schnettler, R. An *in Vitro* Assessment of the Antibacterial Properties and Cytotoxicity of Nanoparticulate Silver Bone Cement. *Biomaterials* **2004**, *25*, 4383–4391.
5. Lee, H. Y.; Park, H. K.; Lee, Y. M.; Kim, K.; Park, S. B. A Practical Procedure for Producing Silver Nanocoated Fabric and Its Antibacterial Evaluation for Biomedical Applications. *Chem. Commun.* **2007**, 2959–2961.
6. Martinez-Castanon, G. A.; Nino-Martinez, N.; Martinez-Gutierrez, F.; Martinez-Mendoza, J. R.; Ruiz, F. Synthesis and Antibacterial Activity of Silver Nanoparticles with Different Sizes. *J. Nanopart. Res.* **2008**, *10*, 1343–1348.
7. Nino-Martinez, N.; Martinez-Castanon, G. A.; Aragon-Pina, A.; Martinez-Gutierrez, F.; Martinez-Mendoza, J. R.; Ruiz, F. Characterization of Silver Nanoparticles Synthesized on Ttitanium Dioxide Fine Particles. *Nanotechnology* **2008**, *19*, Article number: 065711.
8. Trevors, J. T. Silver Resistance and Accumulation in Bacteria. *Enzyme Microb. Technol.* **1987**, *9*, 331–333.
9. Feng, Q. L.; Wu, J.; Chen, G. Q.; Cui, F. Z.; Kim, T. N.; Kim, J. O. A Mechanistic Study of the Antibacterial Effect of Silver Ions on *Escherichia coli* and *Staphylococcus aureus*. *J. Biomed. Mater. Res.* **2000**, *52*, 662–668.

10. Panacek, A.; Kvitek, L.; Prucek, R.; Kolar, M.; Vecerova, R.; Pizurova, N.; Sharma, V. K.; Nevecna, T.; Zboril, R. Silver Colloid Nanoparticles: Synthesis, Characterization, and Their Antibacterial Activity. *J. Phys. Chem. B* **2006**, *110*, 16248–16253.
11. Morones, J. R.; Elechiguerra, J. L.; Camacho, A.; Holt, K.; Kouri, J. B.; Ramirez, J. T.; Yacaman, M. J. The Bactericidal Effect of Silver Nanoparticles. *Nanotechnology* **2005**, *16*, 2346–2353.
12. Sondi, I.; Salopek-Sondi, B. Silver Nanoparticles As Antimicrobial Agent: a Case Study on *E. coli* As a Model for Gram-Negative Bacteria. *J. Colloid Interface Sci.* **2004**, *275*, 177–182.
13. Choi, O.; Deng, K. K.; Kim, N. J.; Ross, L.; Surampalli, R. Y.; Hu, Z. Q. The Inhibitory Effects of Silver Nanoparticles, Silver Ions, and Silver Chloride Colloids on Microbial Growth. *Water Res.* **2008**, *42*, 3066–3074.
14. Madhumathi, K.; Kumar, P. T. S.; Abhilash, S.; Sreeja, V.; Tamura, H.; Manzoor, K.; Nair, S. V.; Jayakumar, R. Development of Novel Chitin/Nanosilver Composite Scaffolds for Wound Dressing Applications. *J. Mater. Sci. Mater. Med.* **2010**, *21*, 807–813.
15. Sureshkumar, M.; Siswanto, D. Y.; Lee, C. K. Magnetic Antimicrobial Nanocomposite Based on Bacterial Cellulose and Silver Nanoparticles. *J. Mater. Chem.* **2010**, *20*, 6948–6955.
16. Yu, D. G.; Teng, M. Y.; Chou, W. L.; Yang, M. C. Characterization and Inhibitory Effect of Antibacterial PAN-Based Hollow Fiber Loaded with Silver Nitrate. *J. Membr. Sci.* **2003**, *225*, 115–123.
17. Chou, W. L.; Yu, D. G.; Yang, M. C. The Preparation and Characterization of Silver-Loading Cellulose Aacetate Hollow Fiber Membrane for Water Treatment. *Polym. Adv. Technol.* **2005**, *16*, 600–607.
18. Taurozzi, J. S.; Arul, H.; Bosak, V. Z.; Burban, A. F.; Voice, T. C.; Bruening, M. L.; Tarabara, V. V. Effect of Filler Incorporation Route on the Properties of Polysulfone-Silver Nanocomposite Membranes of Different Porosities. *J. Membr. Sci.* **2008**, *325*, 58–68.
19. Zodrow, K.; Brunet, L.; Mahendra, S.; Li, D.; Zhang, A.; Li, Q. L.; Alvarez, P. J. J. Polysulfone Ultrafiltration Membranes Impregnated with Silver Nanoparticles Show Improved Biofouling Resistance and Virus Removal. *Water Res.* **2009**, *43*, 715–723.
20. Basri, H.; Ismail, A. F.; Aziz, M.; Nagai, K.; Matsuura, T.; Abdullah, M. S.; Ng, B. C. Silver-Filled Polyethersulfone Membranes for Antibacterial Applications—Effect of PVP and TAP Addition on Silver Dispersion. *Desalination* **2010**, *261*, 264–271.
21. Mauter, M. S.; Wang, Y.; Okemgbo, K. C.; Osuji, C. O.; Giannelis, E. P.; Elimelech, M. Antifouling Ultrafiltration Membranes *via* Post-Fabrication Grafting of Biocidal Nanomaterials. *ACS Appl. Mater. Interface* **2011**, *3*, 2861–2868.
22. Rathod, D.; Dickinson, C.; Egan, D.; Dempsey, E. Platinum Nanoparticle Decoration of Carbon Materials with Applications in Non-Enzymatic Glucose Sensing. *Sens. Actuat. B: Chem.* **2010**, *143*, 547–554.
23. Zhao, Y. C.; Zhan, L.; Tian, J. N. A.; Nie, S. L.; Ning, Z. MnO_2 Modified Multi-Walled Carbon Nanotubes Supported Pd Nanoparticles for Methanol Electro-Oxidation in Alkaline Media. *Int. J. Hydrogen Energy* **2010**, *35*, 10522–10526.
24. Jahjah, M.; Kihn, Y.; Teuma, E.; Gomez, M. Ruthenium Nanoparticles Supported on Multi-Walled Carbon Nanotubes: Highly Effective Catalytic System for Hydrogenation Processes. *J. Mol. Catal. A: Chem.* **2010**, *332*, 106–112.
25. Yuan, W.; Jiang, G. H.; Che, J. F.; Qi, X. B.; Xu, R.; Chang, M. W.; Chen, Y.; Lim, S. Y.; Dai, J.; Chan-Park, M. B. Deposition of Silver Nanoparticles on Multiwalled Carbon Nanotubes Grafted with Hyperbranched Poly(amidoamine) and Their Antimicrobial Effects. *J. Phys. Chem. C* **2008**, *112*, 18754–18759.
26. Li, Z. Z.; Fan, L. J.; Zhang, T.; Li, K. Facile Synthesis of Ag Nanoparticles Supported on MWCNTs with Favorable Stability and Their Bactericidal Properties. *J. Hazard. Mater.* **2011**, *187*, 466–472.
27. Lai, G. S.; Wu, J.; Ju, H. X.; Yan, F. Streptavidin-Functionalized Silver-Nanoparticle-Enriched Carbon Nanotube Tag for Ultrasensitive Multiplexed Detection of Tumor Markers. *Adv. Funct. Mater.* **2011**, *21*, 2938–2943.
28. Murugan, E. M. E.; Vimala, G. Effective Functionalization of Multiwalled Carbon Nanotube with Amphiphilic Poly(propyleneimine) Dendrimer Carrying Silver Nanoparticles for Better Dispersability and Antimicrobial Activity. *J. Colloid Interface Sci.* **2011**, *357*, 354–365.
29. Sahoo, S. S. S.; Husale, S.; Karna, S.; Nayak, S. K.; Ajayan, P. M. Controlled Assembly of Ag Nanoparticles and Carbon Nanotube Hybrid Structures for Biosensing. *J. Am. Chem. Soc.* **2011**, *133*, 4005–4009.
30. Castle, A. B.; Gracia-Espino, E.; Nieto-Delgado, C.; Terrones, H.; Terrones, M.; Hussain, S. Hydroxyl-Functionalized and N-Doped Multiwalled Carbon Nanotubes Decorated with Silver Nanoparticles Preserve Cellular Function. *ACS Nano* **2011**, *5*, 2458–2466.
31. Lin, Y.; Baggett, D. W.; Kim, J. W.; Siochi, E. J.; Connell, J. W. Instantaneous Formation of Metal and Metal Oxide Nanoparticles on Carbon Nanotubes and Graphene *via* Solvent-Free Microwave Heating. *ACS Appl. Mater. Interface* **2011**, *3*, 1652–1664.
32. Socrates, G. *Infrared Characteristic Group Frequencies*, 2nd ed.; John Wiley & Sons: New York, 2004.
33. Ros, T. G.; van Dillen, A. J.; Geus, J. W.; Koningsberger, D. C. Surface Oxidation of Carbon Nanofibres. *Chem.—Eur. J.* **2002**, *8*, 1151–1162.
34. Wang, L.; Ge, L.; Rufford, T. E.; Chen, J. L.; Zhou, W.; Zhu, Z. H.; Rudolph, V. A Comparison Study of Catalytic Oxidation and Acid Oxidation to Prepare Carbon Nanotubes for Filling with Ru Nanoparticles. *Carbon* **2011**, *49*, 2022–2032.
35. Luo, C. C.; Zhang, Y. H.; Zeng, X. W.; Zeng, Y. W.; Wang, Y. G. The Role of Poly(ethylene glycol) in the Formation of Silver Nanoparticles. *J. Colloid Interface Sci.* **2005**, *288*, 444–448.
36. Qi, X. B.; Poernomo, G.; Wang, K. A.; Chen, Y. A.; Chan-Park, M. B.; Xu, R.; Chang, M. W. Covalent Immobilization of Nisin on Multi-Walled Carbon Nanotubes: Superior Antimicrobial and Anti-Biofilm Properties. *Nanoscale* **2011**, *3*, 1874–1880.
37. Liang, C. Y.; Krimm, S. Infrared Spectra of High Polymers. 7. Polyacrylonitrile. *J. Polym. Sci.* **1958**, *31*, 513–522.
38. Oh, N. W.; Jegal, J.; Lee, K. H. Preparation and Characterization of Nanofiltration Composite Membranes Using Polyacrylonitrile (PAN). II. Preparation and Characterization of Polyamide Composite Membranes. *J. Appl. Polym. Sci.* **2001**, *80*, 2729–2736.
39. Avadanei, M.; Drobota, M.; Stoica, I.; Rusu, E.; Barboiu, V. Surface Morphology and Amide Concentration Depth Profile of Aminolyzed Poly(ethylene terephthalate) Films. *J. Polym. Sci., Part A Polym. Chem.* **2010**, *48*, 5456–5467.
40. Dragan, S.; Grigoriu, G.; Petrariu, I. Cationic Polyelectrolytes. 9. New Aspects of Poly(N,N-Dialkylaminoalkylacrylamides) Synthesis *via* Nitrile Group Reaction of Polyacrylonitrile with N,N-Dialkylaminoalkylamines. *Polym. Bull.* **1991**, *27*, 17–24.
41. Yang, H. L.; Lin, J. C. T.; Huang, C. Application of Nanosilver Surface Modification to RO Membrane and Spacer for Mitigating Biofouling in Seawater Desalination. *Water Res.* **2009**, *43*, 3777–3786.